Involvement of Glutamic Acid 278 in the Redox Reaction of the Cytochrome *c* Oxidase from *Paracoccus denitrificans* Investigated by FTIR Spectroscopy[†]

Petra Hellwig,[‡] Julia Behr,[§] Christian Ostermeier,[§] Oliver-Matthias H. Richter,[∥] Ute Pfitzner,[∥] Annette Odenwald,[∥] Bernd Ludwig,[∥] Hartmut Michel,[§] and Werner Mäntele*[,‡]

Institut für Biophysik, Theodor-Stern-Kai 7 Haus 74, D-60590 Frankfurt/Main, Germany, Max-Planck-Institut für Biophysik, Heinrich-Hoffmann-Strasse 7, 60528 Frankfurt/Main, Germany, and Institut für Biochemie, Molekulare Genetik, Marie-Curie-Strasse 9, 60439 Frankfurt/Main, Germany

Received October 15, 1997; Revised Manuscript Received March 16, 1998

ABSTRACT: The molecular processes concomitant with the redox reactions of wild-type and mutant cytochrome *c* oxidase from *Paracoccus denitrificans* were analyzed by a combination of protein electrochemistry and Fourier transform infrared (FTIR) difference spectroscopy. Oxidized-minus-reduced FTIR difference spectra in the mid-infrared (4000−1000 cm^{-1}) reflecting full or stepwise oxidation and reduction of the respective cofactor(s) were obtained. In the 1800−1000 cm^{-1} range, these FTIR difference spectra reflect changes of the polypeptide backbone geometry in the amide I (ca. 1620−1680 cm^{-1}) and amide II (ca. 1560−1540 cm^{-1}) region in response to the redox transition of the cofactor(s). In addition, several modes in the 1600−1200 cm^{-1} range can be tentatively attributed to heme modes. A peak at 1746 cm^{-1} associated with the oxidized form and a peak at 1734 cm^{-1} associated with the reduced form were previously discussed by us as proton transfer between Asp or Glu side chain modes in the course of the redox reaction of the enzyme [Hellwig, P., Rost, B., Kaiser, U., Ostermeier, C., Michel, H., and Mäntele, W. (1996) *FEBS Lett. 385*, 53−57]. These signals were resolved into several components associated with the oxidation of different cofactors. For a stepwise potential titration from the fully reduced state (−0.5 V) to the fully oxidized state (+0.5 V), a small component at 1738 cm^{-1} develops in the potential range of approximately +0.15 V and disappears at more positive potentials while the main component at 1746 cm^{-1} appears in the range of approximately +0.20 V (all potentials quoted vs Ag/AgCl/3 M KCl). This observation clearly indicates two different ionizable residues involved in redox-induced proton transfer. The major component at 1746 cm^{-1} is completely lost in the FTIR difference spectra of the Glu 278 Gln mutant enzyme. In the spectrum of the subunit I Glu 278 Asp mutant enzyme, the major component of the discussed difference band is lost. In contrast, the complete difference signal of the wild-type enzyme is preserved in the Asp 124 Asn, Asp 124 Ser, and Asp 399 Asn variants, which are critical residues in the discussed proton pump channel as suggested from structure and mutagenesis experiments. On the basis of these difference spectra of mutants, we present further evidence that glutamic acid 278 in subunit I is a crucial residue for the redox reaction. Potential titrations performed simultaneously for the IR and for the UV/VIS indicate that the signal related to Glu 278 is coupled to the electron transfer to/from heme *a*; however, additional involvement of Cu_B electron transfer cannot be excluded.

In the cellular respiration process, oxygen reduction is coupled to the formation of an electrochemical membrane proton gradient that drives ATP synthesis. The terminal heme/copper oxidases in the respiratory electron-transfer chains reduce oxygen to water and efficiently couple electron and proton transfer. Besides the four protons required for water formation (termed scalar protons despite the fact that they originate from the cytoplasmic side of bacteria or matrix side of mitochondria), up to four protons are pumped by most terminal heme/copper oxidases across the membrane (termed vectorial protons) to contribute to the electrochemical proton gradient. Four redox-active cofactors participate in the electron transfer within the cytochrome *c* oxidase. Cu_A represents the first acceptor for electrons from cytochrome *c* that are subsequently transferred to heme *a*. Further electron transfer leads to the binuclear heme copper center (heme a_3 and Cu_B) where oxygen is bound and reduced (for reviews, see refs *1* and *2*).

Two separate channels, one for vectorial and one for scalar protons, have been predicted by mutagenesis experiments in which proton transfer was interrupted whereas oxygen reduction was still possible (*3*, *4*). Recently, the structure of the four-subunit cytochrome *c* oxidase from *Paracoccus denitrificans* has been determined (*5*) as well as that of the 13-subunit cytochrome *c* oxidase from bovine heart mitochondria (*6*, *7*). The structure of the protein suggests possible

[†] Financial support from the Deutsche Forschungsgemeinschaft (SFB 472 to B.L. and H.M. and VDFG1054/17-1 to W.M.), the Max-Planck-Gesellschaft, and the Fonds der chemischen Industrie is gratefully acknowledged.

* Corresponding author phone, 49-69-6301-5835; fax, 49-69-6301-5838; e-mail, MAENTELE@BIOPHYSIK.UNI-FRANKFURT.DE.

[‡] Institut für Biophysik.

[§] Max-Planck-Institut für Biophysik.

[∥] Institut für Biochemie.

S0006-2960(97)02557-9 CCC: $15.00
Published on Web 04/30/1998

proton-transfer pathways, involving residues Asp 124, Thr 203, and Asn 199 in subunit I that could form the entrance of one pathway for protons. From the pathway as proposed for the bacterial enzyme, proton transfer might lead to Glu 278. Beyond this residue, two possibilities are conceivable. Either the protons might be transferred to one of the heme a_3 propionates and then reach the exit pathway. Alternatively, proton transfer to the Cu_B ligand His 325 and then to the exit pathway with Asp 399 as a component, involving a conformational change of the histidine residue upon protonation, is possible (*5*, *8*, *9*). The importance of Asn 199 and Asp 124 for proton-transfer reactions and Glu 278 for enzymatic turnover is indicated by the structural data as well as by spectroscopic studies on native and mutant enzymes (*3*, *4*).

In a previous publication, we have presented the electrochemically induced FTIR[1] and UV/VIS difference spectra (oxidized-minus-reduced) of the cytochrome *c* oxidase from *P. denitrificans* (*10*). Each signal in the FTIR difference spectrum corresponds to individual mode(s) of the cofactor(s) and their site(s) affected by the perturbation, in the present case by a redox reaction induced by an applied electrode potential. The highly sensitive redox-induced FTIR difference spectra describe the reorganization of the redox centers and their protein sites upon electron transfer. Moreover, through the combination of protein electrochemistry and UV/VIS and FTIR difference spectroscopy, individual cofactors can be addressed by selecting the appropriate electrode potential. The sensitivity of FTIR difference spectroscopy allows individual bonds to be monitored in the course of their redox reactions.

In a different approach, Lübben and Gerwert (*11*) obtained FTIR difference spectra of the bo_3 oxidase from *Escherichia coli* by photoreduction and found similar spectra to the ones published by Hellwig et al. (*10*). Several FTIR spectroscopic studies have used photodissociation of CO-poisoned oxidase, mostly focusing on the spectral region between 2000 and 2200 cm^{-1} where the CO mode can be observed. Park et al. (*12*) investigated the spectral region between 1000 and 2150 cm^{-1} of photoinduced FTIR difference spectra of CO-poisoned oxidase from beef heart mitochondria at 13 K. They observed difference signals, which where mostly attributed to heme vibrational modes perturbed by CO dissociation. In a recent publication, Puustinen et al. (*13*) presented FTIR difference spectra in the spectral range between 1300 and 3200 cm^{-1} of the bo_3 oxidase from *E. coli* after photodissociation of CO. Difference signals at 1731/1724 cm^{-1} were assigned to Glu 278 and correlated to Cu_B redox reactions.

While the previous paper (*10*) was able to demonstrate protein microconformational changes upon complete oxidation/reduction, an attribution to individual electron-transfer steps and an assignment of the protonation reactions to individual residues have not been possible. In the present paper, we use potential titrations to select the redox reactions of individual cofactors for the attribution of proton-transfer steps to individual redox reactions in the enzyme. Difference signals in the spectral region from 1760 to 1720 cm^{-1} have been previously discussed as proton transfer between Asp and Glu side chains in the course of the redox reaction (*10*). We now have resolved this difference signal into several components by a stepwise potential titration from the fully reduced to the fully oxidized state.

For the assignment of the FTIR difference signal at 1746/1734 cm^{-1}, we investigated selected site-directed mutants of subunit I Asp and Glu side chains. The following mutants were selected: Glu 278 Gln, Glu 278 Asp, Asp 124 Asn, Asp 124 Ser, and Asp 399 Asn. These residues were proposed to be involved in proton transfer from the structural data (*5*) and by the effect of mutagenesis experiments on the proton pumping activity (*3*, *4*, *14*).

MATERIALS AND METHODS

Sample Preparation. Cytochrome *c* oxidase from *Paracoccus denitrificans* was prepared as described for the crystallization procedure (*15*). For spectroelectrochemistry, cytochrome *c* oxidase solubilized in *n*-decyl-β-D-maltopyranoside/200 mM phosphate buffer (pH 6.9) and containing 100 mM KCl was concentrated to approximately 0.5−1 mM using Microcon ultrafiltration cells (Amicon, Witten). Exchange of ^1H_2O against ^2H_2O was performed by repeatedly concentrating the enzyme and rediluting it in a ^2H_2O buffer. $^1H/^2H$ exchange was found better than 80% as judged from the shift of the amide II mode at 1550 cm^{-1} in the FTIR absorbance spectra (data not shown). For buffer exchange, the sample was diluted 1:100 in the required buffer (200 mM cacodylate buffer for pH 4.7 and pH 6; 200 mM borate buffer for pH 8 and pH 8.7) and reconcentrated in Microcon ultrafiltration cells.

Mutants. Mutants in the *cta*DII gene (coding for subunit I) were generated as detailed in Pfitzner et al. (*14*), expressed in a *Paracoccus* host strain inactivated in both the heme aa_3 and the cbb_3 oxidase, and purified according to Kleymann et al. (*16*). The wild-type and mutant enzymes were analyzed for enzymatic turnover according to Witt et al. (*17*). Activity was found to be 2% for Glu 278 Gln, 60% for Glu 278 Asp, 5% for Asp 124 Asn, 7% for Asp 124 Ser, and 110% for Asp 399 Asn. The specific heme content of mutants corresponded to that of wild-type, and proton pumping measurements in intact cells (*14*) for mutants Glu 278 Asp and Asp 399 Asn exhibited wild-type characteristics.

Electrochemistry. The ultrathin spectroelectrochemical cell for the UV/VIS and IR was used as previously described (*18*, *19*). Sufficient transmission in the entire 1800−1000 cm^{-1} range, even in the region of strong water absorbance at 1645 cm^{-1}, was achieved with the cell path length set to 6−8 μm. The gold grid working electrode was chemically modified by a 2 mM cysteamine solution for 1 h and then carefully washed with deionized water. Alternative modification with 4,4′-dithiodipyridine, polymerized methyl viologen or pyridine-3-carboxaldehyde thiosemicarbazone (PATS-4) was also attempted. To accelerate the redox reaction, mediators (for composition see Table 1) were added to a final total concentration of 40 μM each. At this concentration and with the path length below 10 μm, no spectral contributions from the mediators in the VIS and IR range could be detected in control experiments with samples lacking the protein, except for the PO modes of the phosphate buffer between 1200 and 1000 cm^{-1}. As a supporting electrolyte, 100 mM KCl was added. Approximately 5−6 μL of the protein solution was sufficient to fill the spectro-

[1] Abbreviations: IR, infrared; FTIR, Fourier transform infrared; SHE, standard hydrogen electrode; VIS, visible.

Table 1: List of Mediators Used for Electrochemistry

compound	E_m [mV] vs Ag/AgCl	ref
ferrocenyltrimethylammoniumiodide	437	29
1,1'-dicarboxylferrocene	436	32
diethyl-3-methylparaphenylendiamine	150	30
ferricyanide	216	31
dimethylparaphenylendiamine (DMPPD)	163	30
1,1'-dimethylferrocene	133	31
tetramethylparaphenylendiamine (TMPPD)	62	30
tetrachlorobenzochinone	72	31
2,6-dichlorophenolindophenol	9	32
ruthenium hexamine chloride	−8	31
1,2-naphthoquinone	−63	31
trimethylhydroquinone	−108	31
menadione	−220	31
2-hydroxy-1,4-naphthoquinone	−333	31
anthraquinone-2-sulfonate	−433	31
benzyl viologen	−568	32
methyl viologen	−654	32

electrochemical cell. Potentials quoted with the data refer to the Ag/AgCl/3 M KCl reference electrode; add +208 mV for SHE potentials.

Spectroscopy. FTIR and UV/VIS difference spectra as a function of the applied potential were obtained simultaneously from the same sample with a setup combining an IR beam from the interferometer for the 4000−1000 cm^{-1} range and a dispersive spectrometer for the 400−900 nm range as reported previously (*19*, *21*). First, the protein was equilibrated with an initial potential at the electrode, and single beam spectra in the VIS and IR range were recorded. A potential step to the final potential was then applied, and single beam spectra of this state were again recorded after equilibration. Difference spectra as presented here were then calculated from the two single beam spectra with the initial single beam spectrum taken as reference. No smoothing or deconvolution procedures were applied. The equilibration process for each applied potential was followed by monitoring the electrode current and by successively recording spectra in the visible range until no further changes were observed. The equilibration generally took less than 10 min under the conditions (electrode modification, mediators) reported for the full potential step from −0.5 to 0.5 V. Typically, 128 interferograms at 4 cm^{-1} resolution were co-added for each single beam IR spectrum and transformed using triangular apodization.

RESULTS AND DISCUSSION

Oxidized-Minus-Reduced FTIR Difference Spectra in ^1H_2O and in ^2H_2O. The oxidized-minus-reduced FTIR difference spectrum of *P. denitrificans* cytochrome *c* oxidase obtained for a potential step from −0.5 to +0.5 V (vs Ag/AgCl/3 M KCl) is shown in Figure 1a. Numerous distinct sharp bands appear throughout the spectrum, with half-widths typically below 5−10 cm^{-1} (with the exception of the strong difference signal at 1160 and 1088 cm^{-1}). Comparison of the "forward" (−0.5 to +0.5 V) and the "reverse" (+0.5 to −0.5 V) spectrum, presented in a previous publication (*10*), which are exact mirror images, indicates the full reversibility of the molecular changes induced by the electrochemical redox reaction. No smoothing, deconvolution, or interactive (i.e., weighted) subtractions were applied. Reversibility is even evident for minute bands such as the signals at 1680−1710

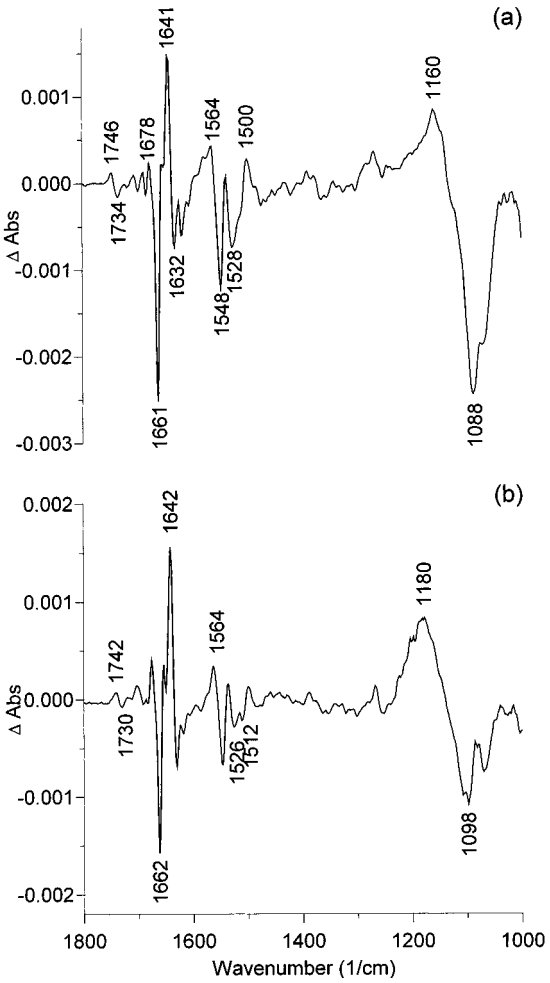

FIGURE 1: Oxidized-minus-reduced FTIR difference spectra of wild-type cytochrome *c* oxidase from *Paracoccus denitrificans* equilibrated in ^1H_2O buffer (a) and in ^2H_2O buffer (b) obtained for a potential step from −0.5 to 0.5 V (vs Ag/AgCl/3 M KCl). Conditions: approximately 0.5 mM cytochrome *c* oxidase in 200 mM phosphate buffer pH 7 (a) or p^{2}H 7 (b) with 100 mM KCl as electrolyte and mediators at a total concentration of 40 μM (for composition, see Materials and Methods). 128 interferograms were co-added for each single beam spectrum; spectral resolution was 4 cm^{-1}.

cm^{-1}. The noise level in these difference spectra can be estimated at frequencies above 1750 cm^{-1}, where no signals appear, to be around 25−50 × 10^{-6} absorbance units. Only in regions of strong absorbance of the sample, such as around 1650 cm^{-1} (water OH modes and amide I) the noise level is slightly higher, though never exceeding 0.1 × 10^{-3} absorbance units. These noise levels are confirmed by "blank" difference spectra calculated from two single beam spectra recorded at the same electrode potential or after a potential cycle (−0.5 to +0.5 V followed by +0.5 to −0.5 V) (data not shown). Thus, the "level of confidence" in these difference spectra extends to even very weak bands.

In line with previous work on IR difference spectroscopy from this and other groups, a reasonable working scheme for the interpretation of FTIR difference spectra generated by a sample perturbation is that each difference signal corresponds to individual mode(s) of the cofactor(s) and their site(s) affected by the perturbation, in the present case by a redox reaction induced by an applied electrode potential. For the cytochrome *c* oxidase, this view allows modes from the heme(s), the copper ligands, the polypeptide backbone, amino

acid side chains, or water molecules to contribute to the spectrum. Signal contributions in the spectral range from 1800 to 1200 cm^{-1} from mediators and the surface modifier can be excluded because of the choice of experimental conditions, i.e., low concentration of mediators (see Materials and Methods). This statement was confirmed by recording blank difference spectra without protein (data not shown).

The electrochemically induced FTIR difference spectra in Figure 1a are essentially identical to the difference spectrum previously reported (*10*), except for the region between 1200 and 1050 cm^{-1} where PO modes from the phosphate buffer indicate proton uptake/release of the enzyme in the course of the redox reaction. A thorough description of the difference bands in the main spectral regions of 1680−1620, 1560−1520, and 1520−1000 cm^{-1} as well as of the region above 1700 cm^{-1} has been given in ref *10*. Briefly, the most prominent bands in the 1680−1620 cm^{-1} region are clearly within the range of the amide I mode absorbance from the polypeptide backbone, and an assignment of the difference signals at 1661 and 1641 cm^{-1} to small alterations of the secondary structure elements upon the redox reaction appears reasonable. The small amplitude of these signals, however, precludes sizable conformational changes and suggests that only a few amide modes are affected by the redox reaction. An alternative assignment of some of these strong signals to heme modes, in particular to the heme formyl group, should be considered and cannot be ruled out at present.

For the signals in the adjacent region between 1560 and 1520 cm^{-1}, a straightforward assignment to amide II modes was considered but appears less probable since little or no shift for $^1H/^2H$ exchange was observed, and contributions from aromatic amino acid side chains were thus taken into account. Beyond contributions from amide II modes and from aromatic amino acid side chains, this region could also include contributions from the antisymmetric COO^- modes caused by proton uptake/release of COOH groups.

In the region above 1680 cm^{-1}, only small signals are present. The most pronounced ones are a negative signal at 1734 cm^{-1} and a positive signal of comparable intensity at 1746 cm^{-1}. According to the convention used here, the negative signal at 1734 cm^{-1} is associated with the reduced form at −0.5 V, while the positive signal at 1746 cm^{-1} is associated with the oxidized form at +0.5 V. These signals were previously assigned to the C═O mode(s) of aspartic or glutamic acid side chains and attributed to the protonations/deprotonations of carboxylic groups in the redox process. This assignment was based on the frequency of the signal, which is in the typical range for Asp/Glu side chain groups in proteins: 1720−1760 cm^{-1} (*22*−*24*). In addition to the frequency of the signal, its half-width (fwhm $\approx$ 10 cm^{-1}) supports attribution to a carboxyl group buried within the protein rather than to a group on the surface, which would appear at lower frequency (toward 1700 cm^{-1}) due to hydrogen bonding but also appear broader because of the conformational flexibility of a surface group. The strongest argument for an assignment to an Asp or Glu side chain carboxyl group, however, was provided by Hellwig et al. (*10*) on the basis of preliminary $^1H_2O/^2H_2O$ substitution experiments, which showed a clear 4−5 cm^{-1} downshift upon $^1H/^2H$ exchange both for the 1746 cm^{-1} component and for the 1734 cm^{-1} component.

Figure 1b shows the full-size oxidized-minus-reduced FTIR difference spectrum of the cytochrome *c* oxidase equilibrated in ^2H_2O buffer obtained for a potential step from −0.5 to +0.5 V. About 80% $^1H/^2H$ exchange was obtained after resuspension of the concentrated enzyme in ^2H_2O and extended equilibration for over 3 weeks at 4 °C as judged from the disappearance of the amide II mode in the absorbance spectrum at 1550 cm^{-1} (data not shown). The difference spectrum in ^2H_2O shows comparable spectral features as the one in ^1H_2O, with a number of small but characteristic frequency shifts and some additional intensity changes. The major signals in the amide I region are almost unaffected by deuteration and shift by only 1−2 cm^{-1} as expected for amide I modes (predominantly C═O vibrations) in an α-helical secondary structure. As mentioned above, the general feature of the signals in the 1560−1520 cm^{-1} region is little changed in ^2H_2O, only the band pattern at 1528 cm^{-1} changes, which makes assignment of these bands to amide II modes rather unlikely. With the exception of a band at 1706 cm^{-1} which gets stronger in ^2H_2O, a decrease of the signal at 1686 cm^{-1}, and some alterations of the small bands between 1705 and 1680 cm^{-1}, the shift of the difference feature at 1746/1734 cm^{-1} (^1H_2O) to 1742/1730 cm^{-1} (^2H_2O) remains the only noticeable effect of ^2H_2O.

FTIR Difference Spectra of Stepwise Oxidation. The difference spectra presented in Figure 1 were generated by a full oxidative (−0.5 to +0.5 V) step and should thus represent the sum of molecular changes induced by the redox reactions of all cofactors. To discern molecular changes from individual cofactors, a stepwise oxidation was performed. Figure 2 shows FTIR difference spectra obtained for different potential steps in the 1720−1760 cm^{-1} region, which comprises signals from Asp and Glu side chain carboxyl groups. All potential steps were started from the fully reduced state obtained through equilibration at an electrode potential of −0.5 V. Raising the potential from −0.5 to 0 V and from −0.5 to 0.1 V results in a baseline (Figure 2a, dotted line and thin-solid line) with none of the signals exceeding the noise level of approximately $10-20 \times 10^{-6}$ absorbance units. Raising the potential from −0.5 to +0.15 V (dashed−dotted line) results in a difference spectrum with a negative lobe at 1728 cm^{-1} and a positive lobe at 1738 cm^{-1}, both with amplitudes clearly exceeding the noise level. These two signals correspond to the loss of COOH absorption of a group absorbing in the reduced state at 1728 cm^{-1} and to the gain of COOH absorbance of a group absorbing in the oxidized state at 1738 cm^{-1}. Both the positive and the negative part of this difference signal are large enough to correspond to individual COOH groups, and a reasonable scenario appears to be the transfer of a proton from one group to the other group.

An unexpected feature is seen when the potential is raised from −0.5 V to higher potentials, such as to +0.35 (dashed line) or to +0.5 V (thick-solid line). The positive band at 1738 cm^{-1} seen for the −0.5 to +0.15 V potential step has disappeared and is replaced by the band at 1746 cm^{-1}, which was already discussed for full oxidation/full reduction in Figure 1 and by Hellwig et al. (*10*). Partly, this signal is already present as a shoulder of the 1738 cm^{-1} band for the −0.5 to +0.15 V step, indicating an intermediate state between the two potentials (+0.15 and +0.35 V, respectively). The negative band at 1728 cm^{-1} (at 0.15 V) shifts

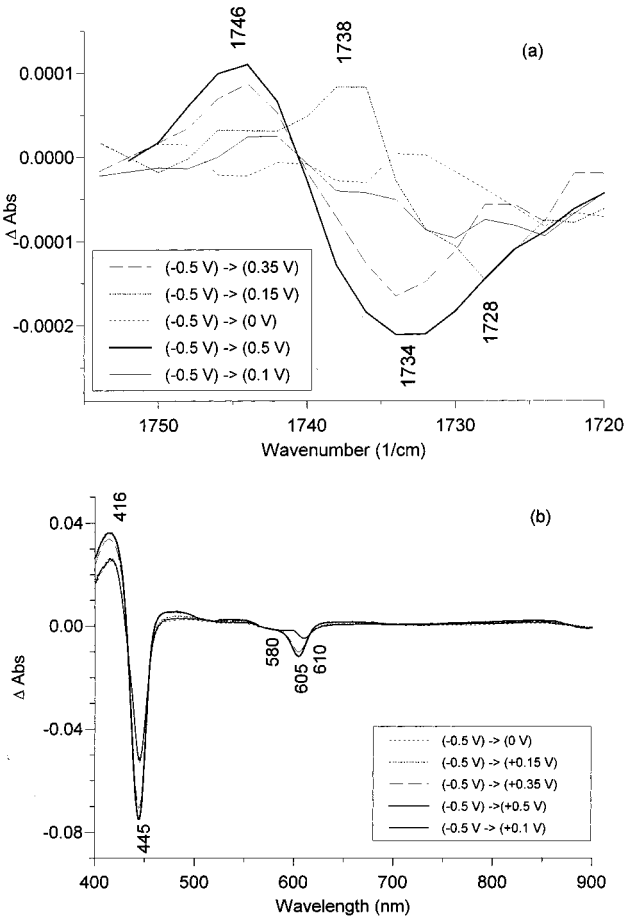

FIGURE 2: FTIR (a) and UV/VIS (b) difference spectra of wild-type *Paracoccus denitrificans* cytochrome *c* oxidase for a stepwise increase of the applied potential. The potential steps indicated are from the reference potential −0.5 to 0 V (thin-dotted line), from −0.5 to +0.1 V (thin line), from −0.5 to +0.15 V (dashed−dotted line), from −0.5 to +0.35 V (dashed line), and from −0.5 to +0.5 V (thick-solid line). Conditions as in Figure 1a.

to 1734 cm^{-1} upon raising the potential to 0.35 V and develops further as presented for the full potential step to 0.5 V in Figure 1a. The difference between raising the potential from −0.5 to +0.35 V and raising it from −0.5 to +0.15 V apparently consists of the loss of the positive peak absorbing at 1738 cm^{-1} and the gain of the positive peak absorbing at 1746 cm^{-1}. This loss should manifest itself in a decrease of absorption (i.e., a negative signal) for the disappearing 1738 cm^{-1} peak, which might account for the shift of the minimum from 1728 to 1734 cm^{-1}.

As for the difference signal with the negative band at 1728 cm^{-1} and the positive band at 1738 cm^{-1}, both the integrated absorption of the negative band at 1734 cm^{-1} and of the positive band at 1746 cm^{-1} could well correspond to individual COOH modes. Again, a reasonable scenario would be transfer of a proton from one group to the other group. In the described case, two residues should then be involved in the 1746/1734 cm^{-1} signals for the full potential step to 0.5 V, and two residues are involved in the 1738/1728 cm^{-1} difference band for the potential step to 0.15 V. An alternative possibility would be to consider **one** protonable residue that experiences a shift of its C═O frequency through a change of its local environment, e.g., by assuming different side chain conformations. In this case, both the negative band at 1734 cm^{-1} and the positive band at 1746 cm^{-1} would arise from this one residue, and equally the 1728/1738 cm^{-1} bands might be caused by one (other) residue. The two signals observed for each potential indicate that at least two Asp or Glu side chains change their p*K* values and/or conformations. We shall address this point again below.

It is clear that the signals reported here are induced by electron transfer, as evident from the dependence on the applied potential. Figure 2b shows the difference spectra in the visible spectral range recorded simultaneously to the infrared difference spectra in Figure 2a. In the difference spectrum for the potential step from −0.5 to 0 V, a positive peak at 416 nm and a negative peak at 445, 580, and 610 nm can be observed. These signals have been previously assigned to contributions of heme a_3 (*25*). Studies on model compounds (*28*) showed that these signals are characteristic for high spin centers coordinated by five ligands such as heme a_3. Raising the potential to 0.1 and then to 0.15 V causes no further changes of these signals. In the potential range between 0 and 0.1 V, redox transitions from Cu_A can be expected (*26*) due to its midpoint potential close to the midpoint potential of cytochrome *c* at 45 mV (*18*). The oxidation of Cu_A can be observed in the characteristic spectral range of Cu_A (*33*, *34*) from 700 to 900 nm (data not shown). For the potential step to 0.35 V, an increase of the positive signal at 416 nm and of the negative signal at 445 nm can be seen. The difference signal at 610 nm increases and shifts to 605 nm. These changes can be attributed to the oxidation of heme *a*. Upon raising the potential to 0.5 V, no further changes can be observed.

From these data, we attribute the 1746/1734 cm^{-1} spectral changes (Figure 2a) to electron transfer to/from heme *a*. In view of the fact that Cu_B does not show detectable signals in the UV/VIS range and that redox transitions of this cofactor might be involved, a contribution of Cu_B to these IR difference signals cannot be definitely excluded. The dependence of the IR signals on the potential allows us to exclude heme *a* and a_3 to correlate to the positive signal at 1738 cm^{-1} observed for the potential step from −0.5 to 0.15 V. An assignment of this difference signal to Cu_A is unlikely since the oxidation of this cofactor can already be expected due to its midpoint potential for the potential step from −0.5 to 0.1 V, whereas in the corresponding infrared difference spectra no significant changes can be seen. From these data, we want to assign tentatively the positive signal at 1738 cm^{-1} in Figure 2a to Cu_B electron transfer. (A further correlation of the COOH signals in the 1720−1750 cm^{-1} range to all cofactors present, however, is beyond the scope of this paper.) The reason for this cautious treatment of the present data is the presently unclear role of protonation states for the precise midpoint potentials of the cofactors as well as the influence of the interactions between the cofactors on the midpoint potentials (*25*, *26*).

FTIR Difference Spectra of Mutants. A possible strategy for assignment of IR signals in difference spectra is the use of site-directed mutants. In the case presented here, the replacement of a ionizable residue by a nonionizable one (Asp → Asn, Glu → Gln) appears straightforward, although it bears the clear risk that the removal of a charge can seriously affect the local electrostatic potential. We therefore also used mutants where the local electrostatic potential was maintained as far as possible.

For the assignment of FTIR signals, we have selected the following mutants, where the ionizable residues are replaced by nonionizable groups: Glu 278 Gln, Asp 124 Asn, Asp 124 Ser, and Asp 399 Asn. To avoid perturbations of the electrostatic potential in the protein by neutralizing charged residues, we have further selected the mutation of Glu 278 to Asp. Asp 124, located close to the cytoplasmatic surface, was proposed to be part of a proton-transfer pathway of the cytochrome *c* oxidase from *P. denitrificans*. This pathway was originally suggested to be used for the pumped protons. Glu 278 was proposed to be a part of the same proton-transfer pathway close to heme a_3. Finally, we examined the residue Asp 399. This residue is located near one of the heme a_3 propionates and might contribute to proton exit.

Figures 3 and 4 present the oxidized-minus-reduced FTIR difference spectra of wild-type, Asp 124 Asn, Asp 399 Asn, Glu 278 Gln, and Glu 278 Asp mutant enzymes for a potential step from −0.5 to +0.5 V. Because of slightly different sample concentrations, the spectra of the native and mutant enzyme were normalized for the α-band difference signal in the UV/VIS spectral range. Reduced-minus-oxidized and oxidized-minus-reduced (data not shown) FTIR difference spectra indicate fully reversible and quantitative electrochemistry for the wild-type and all mutants. The reduced proton and electron transfer rates of the mutants (see Materials and Methods) do not affect the spectroscopic and electrochemical properties of the enzymes. In the spectro-electrochemical experiments described here, the cofactors could be oxidized and reduced reversibly even if a kinetically competent proton transfer is not possible, for example, in one of the mutants. Principally, the FTIR difference spectra represent equilibrium states for a given redox state, and a blocked pathway may only be of importance if the equilibration of an internal residue would take an excessively long time.

FTIR spectroscopy is highly sensitive to changes even of individual groups; thus, any alteration in the secondary structure should be monitored in the FTIR difference spectra. This could be, for example, reported by changes in the amide I region (1680−1620 cm^{-1}), where the C═O modes of the polypeptide backbone appear. In the spectral region from 1680 to 1000 cm^{-1}, no significant differences between the native and mutant enzymes (Figures 3 and 4) can be observed, suggesting that the structure remains essentially undisturbed by replacement of the discussed amino acids in the protein. We thus predict from these spectra only minor deviations from the native enzyme structure, possibly too small to be detected by X-ray crystallography at the present resolution. The small differences between the spectra in the 1650 cm^{-1} range can be explained by the high noise level in the region of the water band absorption at 1645 cm^{-1}.

In the spectral region from 1560 to 1520 cm^{-1} (the amide II region), no changes by exchange of specific Asp or Glu residues could be observed confirming the "intact" structure of the mutant enzyme. At approximately *1450−1420* cm^{-1} and *1620−1570* cm^{-1}, difference signals of the symmetric and antisymmetric COO^- modes induced by protonation/deprotonation of COOH groups are expected; however, these contributions are possibly overlapped by other stronger signals. It thus cannot be excluded that the exchange of the COOH residues affects this spectral range.

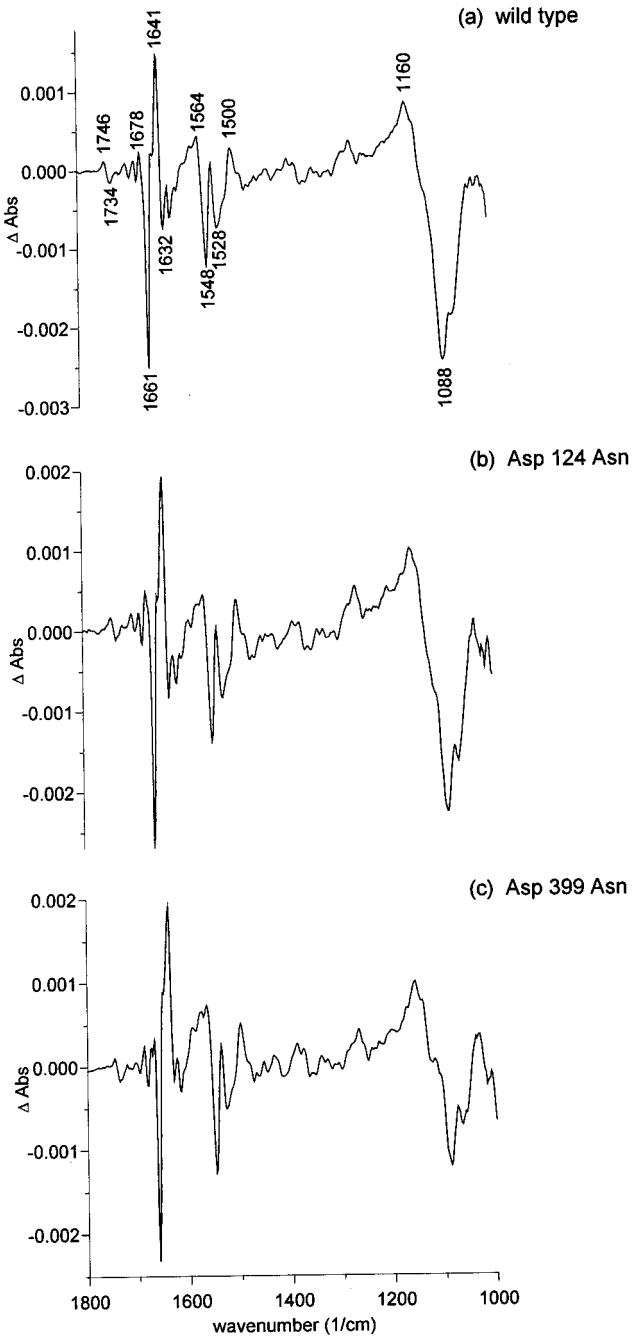

FIGURE 3: Comparison of native (a), Asp 124 Asn mutant (b), Asp 399 Asn mutant (c) cytochrome *c* oxidase from *Paracoccus denitrificans* obtained for a potential step from −0.5 to +0.5 V (vs Ag/AgCl/3 M KCl) from 1800 to 1000 cm^{-1}. Conditions as in Figure 1a.

The lower spectral region from 1200 to 1000 cm^{-1} is dominated by broad signals, a positive one at 1160 cm^{-1} and a negative one at 1088 cm^{-1}. These signals can be observed in the spectra of the wild-type and all mutants. These bands were previously assigned to PO modes caused by protonation changes of the phosphate buffer correlating with the proton uptake/release of the protein and the mediators (*10*).

The oxidized-minus-reduced FTIR difference spectra of wild-type, Asp 124 Asn, Asp 399 Asn, Glu 278 Gln, and Glu 278 Asp mutant enzyme for a potential step from −0.5 to +0.5 V upon $^1H/^2H$ exchange are presented in the expanded view from 1760 to 1720 cm^{-1} in Figures 5a−c

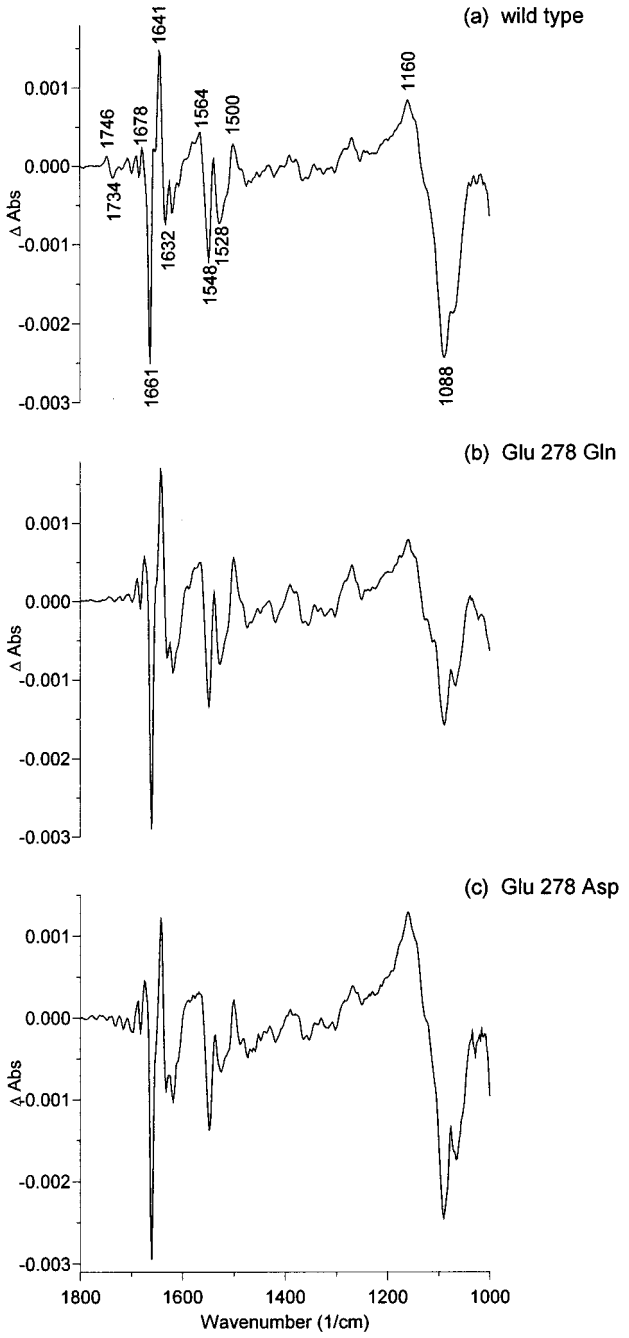

FIGURE 4: Comparison of native (a), Glu 278 Gln mutant (b), and Glu 278 Asp mutant (c) cytochrome *c* oxidase from *Paracoccus denitrificans* obtained for a potential step from −0.5 to +0.5 V (vs Ag/AgCl/3 M KCl) from 1800 to 1000 cm^{-1}. Conditions as in Figure 1a.

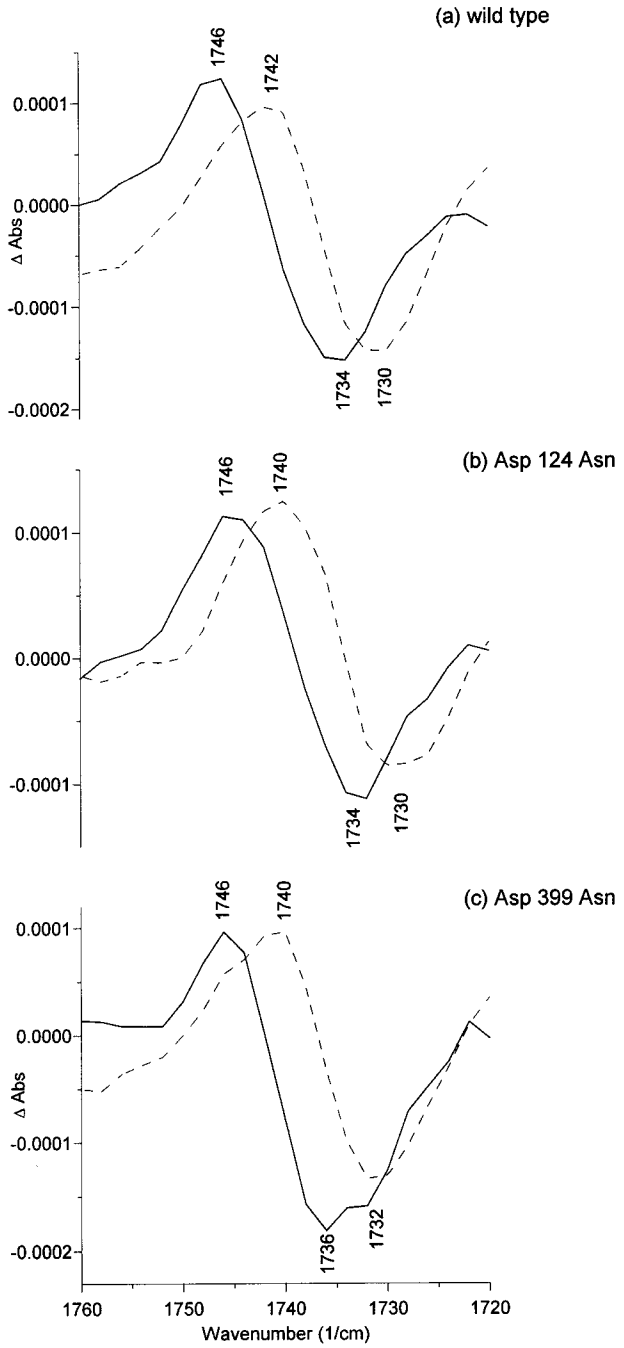

FIGURE 5: Expanded view of the oxidized-minus-reduced FTIR difference spectra in the 1720 to 1760 cm^{-1} range of native (a), Asp 124 Asn mutant (b), and Asp 399 Asn mutant (c) cytochrome *c* oxidase from *Paracoccus denitrificans* obtained for a potential step from − 0.5 to + 0.5 V (vs Ag/AgCl/3 M KCl) equilibrated in ^1H_2O buffer (solid line) and in ^2H_2O buffer (dashed line). Conditions as in Figure 1.

and 6a−c. The sensitivity of the wild-type enzyme to $^1H/^2H$ exchange was already discussed with Figure 1b. From 1680 to 1000 cm^{-1}, the same ^2H sensitivity for the wild type and the mutants can be observed (data not shown).

In the FTIR difference spectrum between approximately 1720 and 1760 cm^{-1}, the C═O double bond of the COOH group from protonated Asp and Glu side chains appears at a position depending on local environment and the hydrogen bonding of the side chain. In this region, the spectra presented show clear differences between the spectra of the wild-type enzyme and some of the mutants.

As shown in Figures 5 and 6, no significant differences between the electrochemically induced FTIR difference spectrum of the wild-type and the Asp 124 Asn mutant protein can be observed for the full potential step from −0.5 to +0.5 V. Although the side chain of Asp 124 is in a critical position in the suggested proton-transfer pathway, it is **clearly not** involved in the 1746/1734 cm^{-1} signals. To support this result, we examined the Asp 124 Ser mutant enzyme (data not shown). Asp 124 Ser shows the same electrochemical and spectroscopic properties as the Asp 124 Asn mutant enzyme, thus confirming these conclusions. In the related Asp 124 Asn and the Asp 124 Ser mutant enzyme in the cytochrome oxidase from *E. coli* (*3*) and from *Rhodo-*

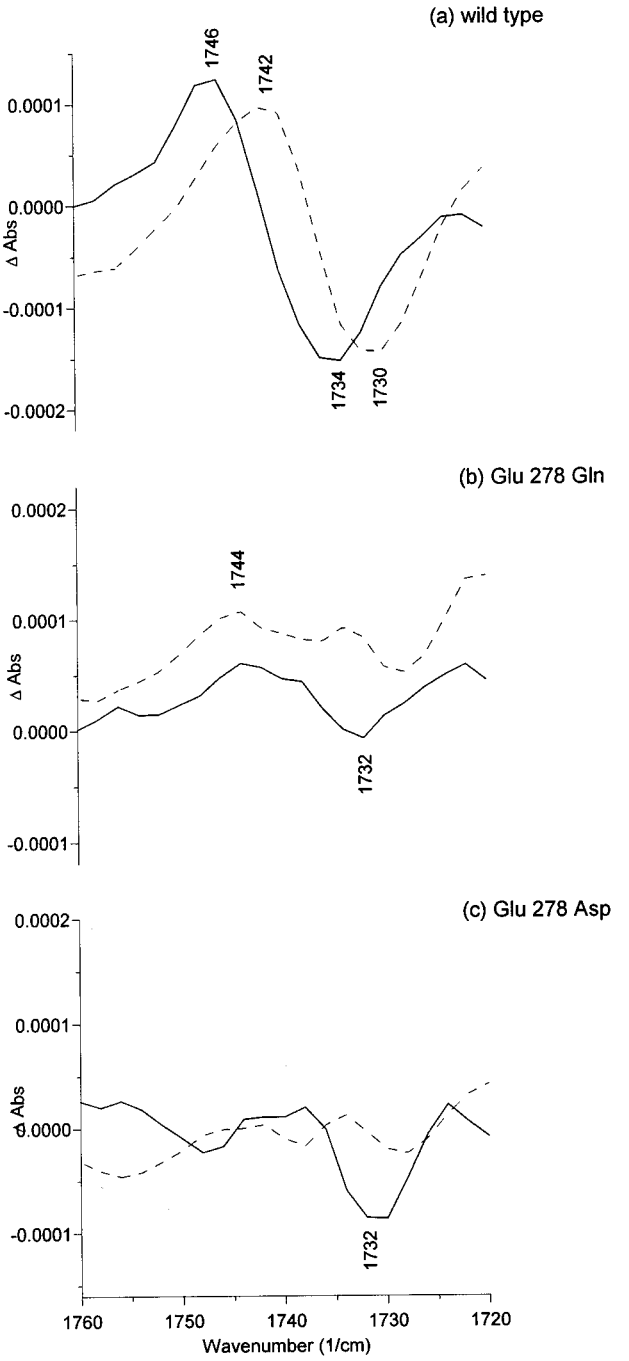

FIGURE 6: Expanded view of the oxidized-minus-reduced FTIR difference spectra in the 1720−1760 cm^{-1} range of native (a), Glu 278 Gln mutant (b), and Glu 278 Asp mutant (c) cytochrome *c* oxidase from *Paracoccus denitrificans* obtained for a potential step from − 0.5 to + 0.5 V (vs Ag/AgCl/3M KCl) equilibrated in ^1H_2O buffer (solid line) and in ^2H_2O buffer (dashed line). Conditions as in Figure 1.

bacter sphaeroides (*4*), the replacement of the side chain results in loss of proton pumping activity; however, some residual enzymatic turnover is retained. Nevertheless, the spectra of the Asp 124 Asn and the Asp 124 Ser mutant enzyme of the *P. denitrificans* cytochrome *c* oxidase seem to be coincident with the spectra of the native protein. We suppose that protons can reach the side chains involved in the proton transfer (e.g., Glu 278) despite the interruption of the transfer way, provided that equilibration is sufficiently long as in the case of the IR experiments presented here.

The electrochemically induced FTIR difference spectra for the full potential step from −0.5 to +0.5 V in Figure 3a−c show a similar difference spectrum for the wild-type and the Asp 399 Asn mutant enzyme. Thus, this residue can be ruled out as a candidate for the difference signal at 1746/1734 cm^{-1}, which is observed for this potential step.

As presented in Figure 5, the Asp 399 Asn and Asp 124 Asn mutant enzymes exhibit the wild-type spectrum in ^2H_2O buffer, in the interesting spectral region from 1760 to 1720 cm^{-1}, thus confirming the results in ^1H_2O.

The electrochemically induced FTIR difference spectra of the wild-type, the Glu 278 Gln, and the Glu 278 Asp mutant enzymes show substantial differences (Figure 4a−c). While the spectrum of the Glu 278 Gln mutant is identical to the spectrum of the native protein in the 1720−1000 cm^{-1} spectral region, the 1746/1734 cm^{-1} signals are almost lost in the spectrum of the mutant enzyme. Only a small residual band with a maximum at 1744 cm^{-1} and a minimum at 1732 cm^{-1} is observed, which probably was hidden under the strong 1746/1734 cm^{-1} signals. In the spectrum of the Glu 278 Asp mutant, the signals at 1746/1734 cm^{-1} decrease in intensity as compared with that of the wild-type protein (see Figure 6).

Figure 6a−c shows the electrochemically induced FTIR difference spectra of the wild-type, Glu 278 Gln, and Glu 278 Asp mutant enzymes after $^1H/^2H$ exchange only for the expanded view from 1760 to 1720 cm^{-1}. In the spectral range from 1760 to 1680 cm^{-1}, the 1740/1730 cm^{-1} signals decrease in the spectra of the Glu 278 Gln and Glu 278 Gln mutant enzyme.

During revision of this manuscript, Puustinen et al. (13) reported FTIR difference spectra of CO-poisoned wild-type, Glu 286 Asp, and Glu 286 Cys mutant enzyme of bo_3 oxidase from *E. coli* at 80 K. Glutamic acid 286 in *E. coli* is the residue homologous to Glu 278 in *P. denitrificans*. Puustinen et al. (*13*) assigned similar difference signals at 1731 and 1724 cm^{-1} (in ^2H_2O) to changes of protonated Glu 286 amino acid as done in this paper. A comparison of the mechanistic implications, however, must be limited because of the different approaches used. While Puustinen et al. (*13*) used the CO molecule as an internal perturbation of the protein, the approach used here as well as that used by Lübben et al. (*11*) aims to direct reduction/oxidation or photoreduction, respectively. Furthermore, it should be considered that the spectra presented in ref 13 were obtained at 80 K. At this temperature, only small conformational changes of the protein can be expected (cf. discussion by Park et al. *12*), and it is not very probable that proton-transfer reactions can occur.

pH dependence of the signals at 1746 cm^{-1} and 1734 cm^{-1}. To examine the pH dependence of the signals at 1746 and 1734 cm^{-1}, oxidized-minus-reduced FTIR difference spectra were recorded at a series of pH values between 4.7 and 9. At lower pH, denaturation of the sample was observed. Spectra at four representative pH values are shown in Figure 7. The positive signal at 1746 cm^{-1} did not show significant alterations upon changing pH, indicating that the p*K* of the group involved is not within the examined pH range. However, the negative signal at 1734 cm^{-1} shows a different behavior. At pH 4.7, the total signal amplitude decreases, indicating the involvement of a group changing its protonation state at pH 4.7 and smaller pH values.

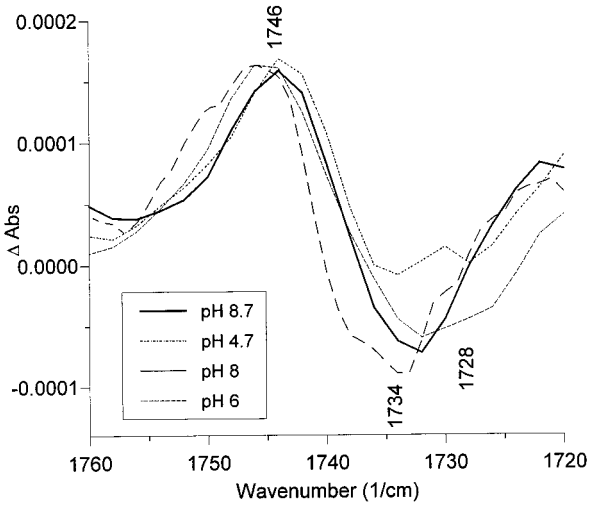

FIGURE 7: pH dependence of the 1746/1734 cm^{-1} difference signal at pH 4.7, 6, 8, and 8.7; for buffers, see Materials and Methods.

For the interpretation of these findings, two scenarios are conceivable. Considering the fact that the amplitudes of both the positive signal at 1746 cm^{-1} as well as the negative signal at 1734 cm^{-1} significantly decrease in the spectra of the Glu 278 Gln and Glu 278 Asp mutant enzymes, both signals might be due to Glu 278.

Together with the results obtained from the spectra recorded at different pH values, this means that Glu 278 might undergo significant environmental changes of the side chain itself upon oxidation of the protein, so that the same group absorbs at 1746 cm^{-1} in the oxidized state and at 1734 cm^{-1} in the reduced state. These environmental changes might be accompanied by a change of the p*K* value of this group. The decrease in the amplitude of the negative signal at 4.7 would indicate a deprotonation of Glu 278 at lower pH arising from pH dependent changes in the direct environment of the Glu 278.

Alternatively, only one of the two signals at 1746 and 1734 cm^{-1} might be due to Glu 278 whereas the other one is caused by another aspartate or glutamate with a different p*K* value. As discussed by Ostermeier et al. (*27*), the structural data suggest that Glu 278 is most likely protonated in the oxidized enzyme. The X-ray crystallographic analysis suggests that Glu 278 is a hydrogen bond donor to the backbone carbonyl oxygen of Met 99. Thus an assignment of the Glu 278 to the positive band at 1746 cm^{-1} is conceivable. The other carboxylic acid might be involved in proton transfer to Glu 278 upon oxidation of the protein.

In the latter case, the mutation of Glu 278 to Gln or Asp might prevent deprotonation of the other group and thus lead to a significant decrease of the corresponding signal or might cause a shift of the corresponding signal possibly leading to an overlap with other signals.

CONCLUSIONS

The data presented here indicate that Glu 278 is involved in at least one of the two signals at 1746 and at 1734 cm^{-1}. Two possibilities are conceivable. First, Glu 278 might be responsible for both the negative and the positive signal in the oxidized-minus-reduced spectrum, assuming a permanently protonated Glu 278 that experiences substantial environmental changes upon redox reaction. Alternatively, only one of the two signals is caused by Glu 278, most likely the positive signal at 1746 cm^{-1} in the oxidized-minus-reduced FTIR spectrum. The negative signal at 1734 cm^{-1} then might be caused by another Asp or Glu, not identified yet, indicating a protonation of Glu 278 and a deprotonation of the second residue upon oxidation of the protein. Moreover, the signals at 1738 and 1728 cm^{-1} obtained from FTIR difference spectra of stepwise oxidation have not been assigned to specific groups yet. Further investigation of other mutant enzymes, the pH dependence of their FTIR difference spectra and their spectral behavior in the course of the redox titration are required in order to identify the groups involved in the signals mentioned.

ACKNOWLEDGMENT

The authors thank Claudia Gries, Frithjof von Germar, and Borries Rost (University Erlangen) for valuable discussions and acknowledge the technical assistance of Werner Müller, Rüdiger Noll, and Hannelore Müller (University of Frankfurt and MPI Frankfurt).

REFERENCES

1. Ferguson-Miller, S., and Babcock, G. T. (1996) *Chem. Rev. 96*, 2889−2907.
2. Babcock, G. T., and Wikström, M. (1992) *Nature 356*, 301−309.
3. Thomas, J. W., Lemieux, L. J., Alben, J. O., and Gennis, R. B. (1993) *Biochemistry 32*, 11173−11180.
4. Garcia-Horsman, J. A., Puustinen, A., Gennis, R. B., and Ferguson-Miller, S. (1995) *Biochemistry 34*, 4428−4433.
5. Iwata, S., Ostermeier, C., Ludwig, B., and Michel, H. (1995) *Nature 376*, 660−669.
6. Tsukihara, T., Aoyama, H., Yamashita, E., Tomizaki, T., Yamaguchi, H., Shinzawa-Itoh, K., Nakashima, R., Yaono, R., and Yoshikawa, S. (1995) *Science 269*, 1069−1074.
7. Tsukihara, T., Aoyama, H., Yamashita, E., Tomizaki, T., Yamaguchi, H., Shinzawa-Itoh, K., Nakashima, R., Yaono, R., and Yoshikawa, S. (1996) *Science 272*, 1136−1144.
8. Morgan, J. E., Verkhovsky, I., and Wikström, M. (1994) *J. Bioenerg. Biomembr. 26*, 599−608.
9. Wikström, M., Bogachev, A., Finel, M., Morgan, J. E., Puustinen, A., Raitio, M., Verkhovskaya, M. L., and Verkhovsky, M. I. (1994) *Biochim. Biophys. Acta. 1187*, 106−111.
10. Hellwig, P., Rost, B., Kaiser, U., Ostermeier, C., Michel, H., and Mäntele, W. (1996) *FEBS Lett. 385*, 53−57.
11. Lübben, M., and Gerwert, K. (1996) *FEBS Lett. 397*, 303−307.
12. Park, S., Pan, L.-P., Chan, S. I., and Alben, J. O. (1996) *Biophys. J. 71*, 1036−1047.
13. Puustinen A., Bailey, J. A., Dyer, R. B., Mecklenburg, S. L., Wikström, M., and Woodruff, W. H. (1997) *Biochemistry 36*, 13195−13200.
14. Pfitzner, U., Odenwald, A., Ostermann, T., Weingard, L., Ludwig., B., and Richter, O.-M. H. (1998) *J. Bioenerg. Biomembr.* (in press).
15. Ostermeier, C., Iwata, S., Ludwig, B., and Michel, H. (1995) *Nat. Struct. Biol. 2*, 842−846.
16. Kleymann, G., Ostermeier, C., Ludwig, B., Skerra, A., and Michel, H. (1995) *Biotechnology 13*, 155−160.
17. Witt, H., Zickermann, V., and Ludwig, B. (1995) *Biochim. Biophys. Acta 1230*, 74−76.
18. Moss, D. A., Nabedryk, E., Breton, J., and Mäntele, W. (1990) *Eur. J. Biochem. 187*, 565−572.
19. Mäntele, W. (1996) in *Biophysical Techniques in Photosynthesis* (Hoff, A. J. and Amesz, J., Eds.) Chapter 9, pp 137−160, Kluwer, Dordrecht.
20. Wikström, M., Harmon, H. J., Ingledew, W. J., and Chance, B. (1976) *FEBS Lett. 65*, 259−277.
21. Mäntele, W. (1993) *Trends Biochem. Sci. 18*, 197−202.

22. Brischwein, M., Scharf, B., Engelhard, M., and Mäntele, W. (1993) *Biochemistry 32*, 13710−13718.
23. Mäntele, W. (1993) in *The Photosynthetic Reaction Center* (Deisenhofer, J., and Norris, J. R., Eds.) Volume II, Chapter 10, pp 239−283, Academic Press, San Diego.
24. Rothschild, K. J. (1992) *J. Bioenerg. Biomembr. 24*, 147−167.
25. Verkhovsky, M. I., Morgan, J. E., and Wikström, M. (1995) *Biochemistry 34*, 7483−7491.
26. Tiesjema, R. H., Muijsers, A. O., and Van Gelder, B. F., (1973) *Biochim. Biophys. Acta 305*, 19−28.
27. Ostermeier, C., Harrenga, A., Ermler, U., and Michel, H. (1997) *Proc. Natl. Acad. Sci. U.S.A. 94*, 10547−10553.
28. *Biological Applications of Resonance Raman Spectroscopy* (Spiro, T., Ed.) Wiley & Sons, New York.
29. Dodson, E. D., Zhao, X.-J., Caughey, W. S., and Elliot, C. M. (1996) *Biochemistry 35*, 444−452.
30. Lahmer, W. M. (1961) in *Oxidation Potentials*, 2nd ed., Prentice Hall Inc., New York.
31. Baymann, F., Moss, D. A., and Mäntele, W. (1991) *Anal. Biochem. 199*, 269−274.
32. Cowan, J. A. (1993), in *Inorganic Biochemistry; An Introduction* VCH, Weinheim.
33. Lappalainen, P., Aasa, R., Malmström, B. G., and Saraste, M. (1993) *J. Biol. Chem. 35*, 26416−26421.
34. Lappalainen, P., Waltmough, N. J., Greenwood, C., and Saraste, M. (1995) *Biochemistry 34*, 5824−5830.

BI9725576